

Blood Flow Versus Hematocrit in Optimization of Oxygen Transfer to Tissue During Fluid Resuscitation

JAMAL SIAM,¹ MARWA KADAN,¹ RON FLAISHON,² and OFER BARNEA¹

¹Department of Biomedical Engineering, Tel Aviv University, 6997801 Tel Aviv, Israel; and ²Department of Intensive Care & Anesthesiology, Tel Aviv Sourasky Medical Center, and the Sackler School of Medicine, Tel Aviv University, Tel Aviv, Israel

(Received 20 January 2015; accepted 15 July 2015; published online 22 July 2015)

Associate Editor Ajit P. Yoganathan oversaw the review of this article.

Abstract—The effectiveness of fluid resuscitation regimens in hemorrhagic trauma is assessed based on its ability to increase oxygen concentration in tissue. Fluid resuscitation using both crystalloids and colloids fluids, creates a dilemma due to its opposing effects on oxygen transfer. It increases blood flow thereby augmenting oxygen transport but it also dilutes the blood simultaneously and reduces oxygen concentration thereby reducing oxygen transport. In this work we have studied these two opposing effects of fluid therapy on oxygen delivery to tissue. A mathematical model of oxygen diffusion from capillaries to tissue and its distribution in tissue was developed and integrated into a previously developed hemodynamic model. The capillary-tissue model was based on the Krogh structure. Compared to other models, fewer simplifying assumptions were made leading to different boundary conditions and less constraints, especially regarding capillary oxygen content at its venous end. Results showed that oxygen content in blood is the dominant factor in oxygen transport to tissue and its effect is greater than the effect of flow. The integration of the capillary/tissue model with the hemodynamic model that links administered fluids with flow and blood dilution indicated that fluid resuscitation may reduce oxygen transport to tissue.

Keywords—Hemorrhage, Capillary-tissue model, Fluid replacement, Computer simulation, Oxygen delivery.

INTRODUCTION

Hemorrhagic shock is the most frequent medical emergency that trauma care units have to deal with. The World Health Organization report, 2010, states that injuries cause more than 10% of the world's death.²⁶ Several treatment guidelines, such as those of the Advanced Trauma Life Support team (ATLS)¹ and

the British National Institute for Clinical Excellence (NICE),¹⁶ were developed for management of patients with hemorrhagic shock. These guidelines consider fluid therapy to be an essential procedure for restoring hemodynamic stability and oxygen delivery to tissue especially in the pre-hospital care. Despite the debate regarding the benefits and shortcomings of crystalloids and colloids fluids,¹⁷ ATLS guidelines recommend an initial rapid infusion of 1–2 L warmed isotonic electrolyte solutions such as normal saline (NS) and lactated Ringer's solution using boluses of 250 mL. The NICE recommends the use of crystalloid fluid resuscitation in absence of radial pulse in boluses of no more than 250 mL. The patient should then be reassessed and the process repeated until a radial pulse is palpable. In both guidelines the appropriate rate and amount of fluid infusion are not clearly defined. This decision of continuing fluid infusion is generally based on general patient's symptoms such as mean arterial pressure, central venous pressure, urine volume, and blood acidity. These parameters have no clear end points at which fluid therapy should be terminated because they are correlated with global physiological effects of fluid resuscitation. Moreover, these clinical symptoms are not directly correlated with tissue oxygen supply and extraction. Early studies of fluid resuscitation used controlled hemorrhage animal models to evaluate the effect of fluid therapy on the treatment outcomes. Some of these studies found that the use of aggressive fluid therapy, with blood and intravenous isotonic fluid, improved the survival rate, after a severe hemorrhage, compared with no treatment or treatment with blood only.^{23,25} However, several other studies showed that fluid therapy can result in deterioration of the oxygen delivery process. Barnea and Sheffer used mathematical modeling to study the effect of fluid resuscitation on cardiac oxygen

Address correspondence to Jamal Siam, Department of Biomedical Engineering, Tel Aviv University, 6997801 Tel Aviv, Israel. Electronic mail: jsiam@birzeit.edu

balance. They showed that oxygen deficit occurred following fluid infusion that increased the workload of the heart without adequate increase in oxygen supply.² Siam *et al.* showed the existence of a maximal oxygen delivery rate during fluid resuscitation in a controlled hemorrhage scenario. They also showed that continuing fluid infusion beyond this point diminishes the oxygen delivery rate to tissue.²⁴ Other studies focused on the balance between restoring the hemodynamic variables to their normal values and achieving lower values that allow better management of hemorrhage consequences. Some of these studies showed that there is some benefit in allowing a patient to have systemic blood hypotension, especially in the case of active hemorrhage or when there is a risk of re-activating a controlled hemorrhage source. The practice of hypotensive fluid therapy has the general goal of achieving a mean arterial pressure of 40–50 mmHg or a systolic pressure of 80 mmHg. Bickel *et al.*³ and Morrison *et al.*¹⁵ found a significant decrease in mortality with the hypotensive resuscitation strategy. Geeraedts *et al.* recommended keeping treatment at the accident site to the minimal treatment possible, with the goal of maintaining vital signs and providing a rapid transport to a higher level trauma center.

In this paper we investigate the effectiveness of fluid therapy based on direct oxygen transfer to tissue. Several models were developed to study oxygen diffusion into tissue; these models were reviewed and classified, according to the number of supplying microcirculation vessels and topology, into single-vessel models and multi-vessels models.^{6,18} Krogh was a pioneer in the development of single capillary models of tissue oxygen uptake.¹¹ This model considered the skeletal muscle to be composed of a set of parallel isolated cylinders with concentric supplying capillaries. The same structure was then used by other researchers to study oxygen uptake in other types of tissues such as brain²¹ and heart.⁴ Our model extends the Krogh's tissue structure to a cascaded set of Krogh structures and assumes that oxygen exchange can occur among the cascaded structures. Sharan *et al.* developed a mathematical model that used the Krogh's tissue structure and used the steady state diffusion equations, to study oxygen transport from a capillary to the surrounding tissue cylinder. They analyzed the conditions under which the end-capillary partial pressure of oxygen is lower than the mean tissue oxygen pressure.²¹ In our study we solved the dynamic oxygen diffusion equations to obtain the steady state solution for oxygen transfer between capillary and tissue. Furthermore, no assumptions were made regarding the end-capillary pressure. Therefore, the direction of oxygen diffusion at the arterial and venous ends of the capillary was determined by the process of oxygen diffusion along the whole axial length of the capillary-tissue

structure. Li *et al.* developed a non-linear model for capillary-tissue oxygen transport and metabolism. Their study considered an axially distributed capillary-tissue cylindrical model that accounts for oxygen convection in red blood cells and plasma. The model provided estimates of oxygen consumption, extraction, and venous oxygen pressure by fitting model solutions to experimental tracer curves of the regional tissue content or venous outflow.¹³ Dash and Bassingthwaight developed a non-linear four region model, with axially distributed cylindrical tissue structures, to study the simultaneous exchange of oxygen and carbon dioxide in the blood-tissue exchange system of the heart. The model gave a physiologically realistic description of oxygen transport and metabolism in the microcirculation of the heart.⁴ Dash and Bassingthwaight model determined the axial distribution of oxygen into tissue. It was implicitly assumed that the radial distribution of oxygen pressure is uniform. Our study took into account both the axial and radial diffusion components inside the tissue cylinders. Moreover, although Dash and Bassingthwaight observed a possible diffusion of oxygen and other species among neighbor tissue elements, they continued to use the original Krogh boundary condition of no oxygen flux among tissue elements. We included the observation of Dash and Bassingthwaight in our model by introducing boundary conditions that allowed oxygen diffusion between the arterial and venous ends of consecutive and coaxial tissue cylinders. Goldman *et al.* developed a mathematical model to study the effect of decreased oxygen supply on skeletal muscle oxygenation and oxygen consumption during sepsis. In their model they decreased oxygen content and blood flow separately; therefore they did not cover the full range of possible oxygen transport parameters.⁷ In our model we allow simultaneous changes in blood flow and oxygen content.

In this study, hemodynamic and oxygen transfer models were integrated to analyze the simultaneous and contradictory effects of fluid resuscitation on tissue oxygenation. On one hand, the infusion of crystalloids and colloids fluid increases the blood flow and therefore the oxygen delivery rate. On the other hand this fluid infusion dilutes blood and consequently reduces the Hematocrit and the concentration of oxygen in blood. The results of this study may help in determining the best fluid resuscitation strategy based on optimal oxygen supply to tissue.

METHODS

To study the fluid therapy dilemma regarding the relative impact of hematocrit and blood flow, a hemodynamic model of the cardiovascular system was

developed. A model of oxygen transport from capillary to tissue was also developed and the two models were studied separately and eventually integrated, Fig. 1. The hemodynamic study was previously described in detail.²⁴ The capillary-tissue model is described in this paper as well as their integration.

The hemodynamic model represents a 70–75 kg human. It was developed to represent major relevant hemodynamic phenomena during normal, hemorrhage and fluid resuscitation scenarios. It included cardiovascular and interstitial compartments, and accounted for the fluid exchange between them. Bleeding and fluid resuscitation were added to simulate the effect of hemorrhage and fluid treatment on tissue oxygen delivery by blood.

The cardiovascular system model, Fig. 1, was composed of a four-chamber heart, the aorta, seven major vascular beds (coronary, head, upper limbs, celiac and superior mesentery, renal, inferior mesentery, and iliac), and a systemic vein. It also included a lumped representation of the pulmonary circulation. This level of detail can adequately simulate the load, flow, and cardiac output as well as pressure levels at the capillary beds which were required to obtain realistic fluid transfer rate between the intravascular and interstitial compartments. In addition, the model can predict flow distribution to vital and non-vital organs that is important in the analysis of hemorrhage and fluid therapy. The hemodynamic model also contained variables such as oxygen content and partial oxygen pressure at each segment. These variables along with hemodynamic variables were used in the capillary-tissue model.

The tissue-capillary model extended the basic Krogh tissue structure to introduce new important oxygen exchange concepts. The set of the resulting time-dependent equations were solved numerically. Modifications of Krogh's model included both radial and axial oxygen diffusion processes. To account for arterial-end of a capillary that may be in proximity to a venous-end, the boundary conditions were cyclic, i.e., an arterial end of a capillary is assumed to be located in proximity to a venous end of a neighboring capillary. This simulates a colony of vessels rather than a single cylindrical set of vessels. In some models oxygen partial pressure at the venous-end of the capillary was constrained to be equal to oxygen partial pressure in the tissue. In this model, this constrain was not applied. Oxygen partial pressure at the end of the capillary was calculated as a result of delivery and extraction. This change was significant for the calculation of oxygen availability in tissue based on flow and O_2 content at the vessel entrance.

Tissue was modeled by a cascade of identical tissue sample volumes (Fig. 2a), each was assumed to follow the Krogh's symmetrical structure. Each tissue cylinder, with total length L and external radius R_t , was segmented into a set of concentric cylinders of equal radial thickness and axial length (Fig. 2b). In the tissue cylinders the model considered solubility, diffusion and consumption of oxygen. The model describes oxygen transport and diffusion into skeletal muscle and other types of tissues for which Krogh model was used in previous studies²¹ and heart.⁴ Myoglobin effect on oxygen delivery was not included in the model. The

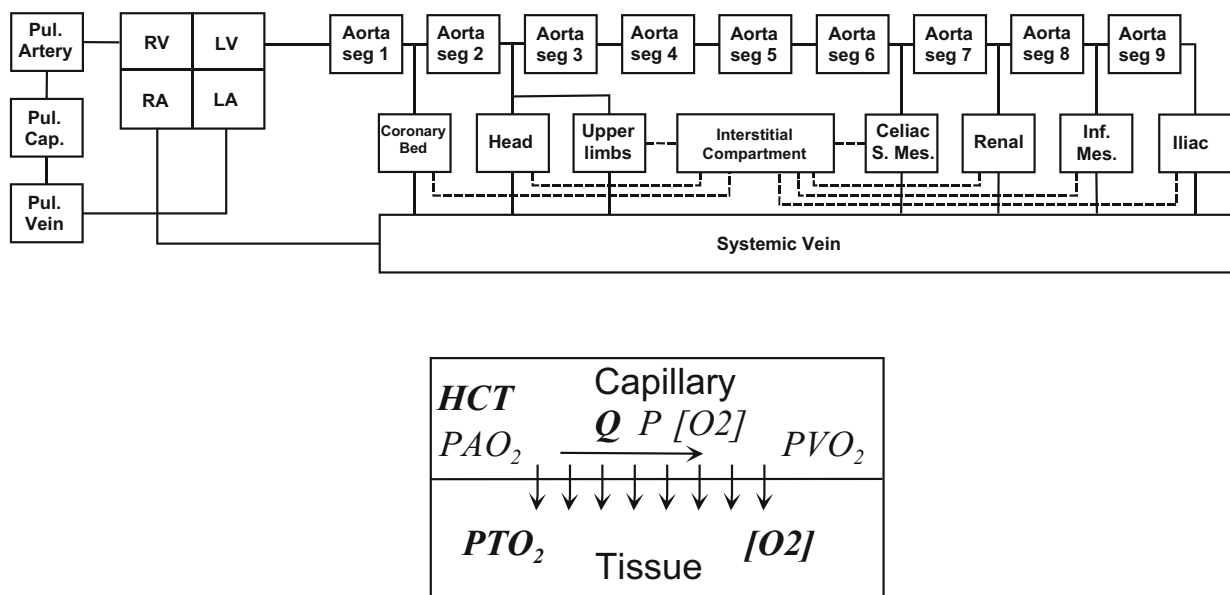


FIGURE 1. Top panel shows the cardiovascular hemodynamic model. Lower panel shows the capillary-tissue model integrated into each capillary bed.

supplying capillary, with radius R_c and length L , was axially segmented in accordance with the axial tissue elements and modeled considering blood velocity, hematocrit, oxygen solubility and dissociation in hemoglobin as well as oxygen radial diffusion through the capillary wall.

Blood oxygen was assumed to diffuse between the capillary and tissue cylinder in the radial direction through a fixed resistance. Oxygen diffusion was assumed to occur in both radial and axial directions in the tissue elements. Oxygen diffusion and solubility coefficients were assumed to be constant in all the tissue segments.

Capillary oxygen, supplied by blood in both dissolved and hemoglobin bound forms, was assumed to be homogeneously distributed in the capillary's radial direction. Accordingly, the capillary total oxygen concentration at any axial position ($C_c(z, t)$) was evaluated from the dissolved and hemoglobin bound components by Eq. (1):

$$C_c(z, t) = \alpha_c P_c(z, t) + HCT \cdot Hb_{RBC} \cdot O_{2Hb} \cdot S_{O_2}(P_c(z, t)), \quad (1)$$

where P_c is the capillary oxygen partial pressure, $S_{O_2}(P_c)$ the oxy-hemoglobin dissociation relation, and α_c , HCT , Hb_{RBC} and O_{2Hb} are the capillary oxygen solubility coefficient, hematocrit, hemoglobin concentration in red blood cells, and oxygen maximum concentration in hemoglobin, respectively. Its inverse was used in the numerical solution to obtain $P_c(z, t)$ using

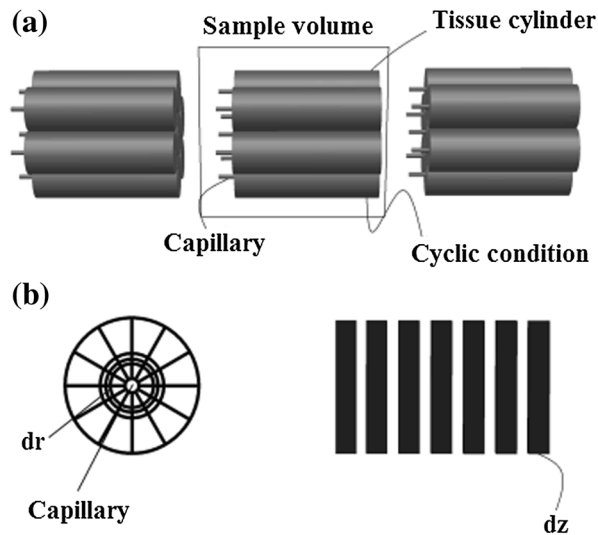


FIGURE 2. Tissue structure was composed of cascaded sample volumes of parallel cylindrical fibers (a). Tissue fiber was segmented in axial and radial directions, while the supplying capillary was axially segmented in accordance with the tissue fiber axial segments (b).

Adair's equation for the oxy-hemoglobin dissociation relation.¹³

During the course of travel from arterial to the venous end of the capillary, oxygen diffuses continuously into tissue in radial direction as shown in the following conservation of mass equation:

$$\pi R_c^2 \cdot \frac{\partial C_c(z, t)}{\partial t} = Q_c \cdot \frac{\partial C_c(z, t)}{\partial z} - 2\pi R_c \cdot J_c(z, t). \quad (2)$$

The diffusion rate (J_c), at any axial location inside the capillary, is proportional to the gradient of oxygen pressure between the blood and tissue across the capillary wall:

$$J_c(z, t) = k_t \cdot (P_c(z, t) - P_t(z, R_c, t)). \quad (3)$$

The coefficient of proportionality (k_t) is the mass transfer coefficient and Q_c is the capillary blood flow. The remaining oxygen flows out of the capillary venous end to the systemic circulation. There is no reason or need to assume that the oxygen partial pressure at the venous end is equal to that of the tissue since maximal extraction is not guaranteed.

In the tissue, oxygen diffusion in a cylinder, assuming axi-symmetric structure, occurs in both axial and radial directions. The governing equations of oxygen diffusion are the conservation of mass equation (Eq. 4) and Fick's law (Eq. 5).¹⁸

$$\alpha_t \frac{\partial P_t}{\partial t} = \alpha_t D_t \left(\frac{\partial^2 P_t}{\partial r^2} + \frac{1}{r} \frac{\partial P_t}{\partial r} \right) + \alpha_t D_t \frac{\partial^2 P_t}{\partial z^2} - M(P_t), \quad (4)$$

$$\begin{cases} J_{t_radial}(z_0, r_0, t) = -\alpha_t D_t \left. \frac{\partial P_t(z, r, t)}{\partial r} \right|_{r=r_0} \\ J_{t_axial}(z_0, r_0, t) = -\alpha_t D_t \left. \frac{\partial P_t(z, r, t)}{\partial z} \right|_{z=z_0} \end{cases}, \quad (5)$$

where $P_t(z, r, t)$ and $J_t(z, r, t)$ are the tissue oxygen partial pressure and the oxygen flux as functions of radial and axial locations. D_t , α_t , z , and r are the tissue oxygen diffusion coefficient, tissue oxygen solubility coefficient, tissue axial coordinate, and radial coordinate, respectively. The function $M(P_t)$ is the oxygen consumption rate per unit volume. In this study, this function is assumed to follow a Michaelis–Menten dynamics (Eq. 6) with the Michaelis–Menten coefficient $K_m = 0.5$ mmHg and maximum consumption rate $M_0 = 8.1 \times 10^{-4}$ (mLO₂/mL s).

$$M(P_t(z, r, t)) = \frac{M_0 \cdot P_t(z, r, t)}{K_m + P_t(z, r, t)}. \quad (6)$$

Boundary conditions, resulting from symmetry assumption, require that oxygen not be exchanged in radial direction among the neighboring tissue cylinders of the same sample volume (Eq. 7).

$$\left. \frac{\partial P_t}{\partial r} \right|_{r=R_c} = 0. \quad (7)$$

The cyclic boundary condition is expressed by Eq. (8):

$$J_{t_axial}(z = L, r, t) = J_{t_axial}(z = 0, r, t). \quad (8)$$

The model also assumed continuity of oxygen flux at the capillary-tissue interface (Eq. 9).

$$J_{t_axial}(z, R_c, t) = J_c(z, t). \quad (9)$$

The dynamic time dependent Eqs. (1)–(6) were solved numerically, using finite difference method, with the boundary conditions in Eqs. (7)–(9), and the initial conditions $C_c(z, 0) = 0.20$ mL O_2 /mL and $P_t(z, r, 0) = 40$ mmHg using MATLAB (The Mathworks, Inc., Natick, MA, USA). Steady state results were obtained from the solution of the time dependent equations. The parameters of the model, listed in Appendix Table 1, were used for the numerical solution. The radius of the capillary and tissue cylinders were assumed to be similar to those used in Ref. 20.

The normal operation steady state capillary-beds blood flow²⁴ were scaled to obtain a normal capillary blood flow $Q_c = 7.7 \times 10^{-9}$ L/s. The same scaling was used to compute the changes in the capillary blood flow (Fig. 3a) during a class III bleeding, stabilization fluid therapy with normal saline, and monitoring phases (Fig. 3). The effects of auto-regulatory processes were ignored as was assumed in Ref. 24.

RESULTS

The hemodynamic model results showed that changes in blood flow and hematocrit affect oxygen delivery.²⁴ Accordingly, these changes affect the oxygen delivery rate into the arterial-end of the capillaries. Figure 3 shows the variations in capillary blood flow, hematocrit and capillary-inlet oxygen delivery rate in class III bleeding (Fig. 3—phase 1), stabilization (Fig. 3—phase 2), fluid resuscitation with saline infusion rates 40, 60, and 80 mL/min (Fig. 3—phase 3), and monitoring phase after cessation of saline infusion (Fig. 3—phase 4). Results showed that capillary blood flow decreased during hemorrhage and increased during fluid resuscitation until it reached a plateau, while hematocrit decreased during all the course of hemorrhage and fluid therapy. This behavior was reflected in a continuously decreasing oxygen delivery rate during bleeding. During fluid resuscitation (phase 3), oxygen delivery rate showed an initial improvement until a maximum point was obtained. Continuing fluid infusion

beyond this point decreased oxygen delivery continuously. Although the hemodynamic and oxygen delivery rate responses were faster for higher infusion rates (Fig. 3), they showed the same trend and achieved the same maximum oxygen delivery rate. Therefore, in the integrated model, we will consider only the case with infusion rate of 80 mL/min to demonstrate the effect of oxygen delivery rate on tissue oxygenation.

Spatial Distribution of Oxygen Pressure and Consumption with Normal Blood Flow and Hematocrit

The steady state response was obtained assuming normal conditions with hematocrit (HCT = 44%) and capillary blood flow ($Q_c = 7.7 \times 10^{-9}$ mL/s). The simulation results showed that the capillary steady state oxygen partial pressure (P_c) was 95.4 mmHg at the inlet of the capillary (Fig. 4c). It decreased quickly at the first quarter-length of the capillary and reached 57.1 mmHg which is about 60% of the total capillary pressure change. The capillary oxygen pressure continued to decrease but with slower rate and reached its minimum (38.4 mmHg) at the axial location of 0.028 cm from the capillary-inlet (arterial-end). Oxygen pressure showed a small increase after this point and reached its final value (39.6 mmHg) at the venous-end. The increase was due to oxygen inflow from tissue to the capillary at the distal segments, resulting from the proximity of the arterial end of the next group of capillaries.

Tissue oxygen partial pressure (P_t) showed a maximum value (77.8 mmHg) at the first tissue element at the inlet of the capillary (Fig. 4a). P_t decreased in the direction of the external radial and the distal axial zones of the tissue cylinder. The minimum value of oxygen pressure (29.7 mmHg) occurred on the external surface of the tissue cylinder at axial distance 0.023 cm from the capillary inlet (76% of the total capillary length). Oxygen levels showed a small continuous increase in axial direction beyond this minimum point in all the radial locations (Fig. 4a). The tissue average oxygen pressure was 40.8 mmHg. Oxygen consumption rate showed a similar behavior to oxygen distribution (Fig. 4b), the maximum consumption rate (8.06×10^{-4} mL O_2 /mL s) occurred at the inlet of the capillary, while the minimum (7.98×10^{-4} mL O_2 /mL s) occurred at the point of tissue minimum oxygen pressure. The tissue mean oxygen consumption rate was 8.015×10^{-4} mL O_2 /mL s.

Tissue Oxygen Pressure and Consumption with Variable Blood Flow and Hematocrit

The steady state tissue average and minimum oxygen pressures, consumption rate, and end-capillary

oxygen pressure were obtained for relative changes in capillary blood flow and hematocrit (Fig. 5). These changes were considered in the range 50% to 100% of the assumed normal values, that is, ($Q_c = 7.7 \times 10^{-9}$ mL/s and $HCT = 44\%$) with a change step of 1%. Figure 5 shows that the relative changes in the tissue and end-capillary oxygen pressure were more sensitive to changes in hematocrit than to blood flow. To better illustrate this behavior, Fig. 6 shows the changes in

average and minimum oxygen pressures as functions of normalized blood flow with constant hematocrit (44%) and of normalized HCT with constant blood flow (7.7×10^{-9} mL/min). In both panels the lines coincide at blood flow and HCT equal 1 that is the point of normal conditions. From that point each variable is reduced independently and its effect on oxygen partial pressure is calculated. Both panels show that holding blood flow constant and reducing HCT results in a

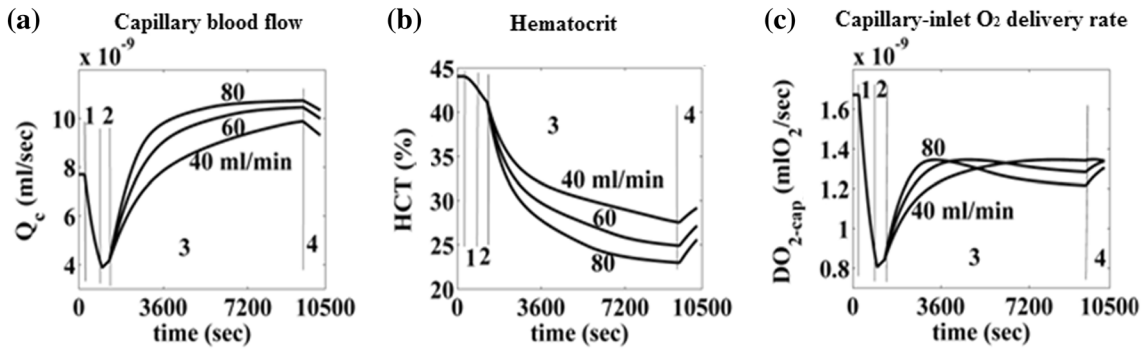


FIGURE 3. Capillary blood flow (a), hematocrit (b) and capillary-inlet oxygen delivery rate (c) during bleeding (1), stabilization (2), fluid therapy with saline (3), and monitoring phases (4), with saline infusion rates 40, 60, and 80 mL/min, as obtained from the integrated hemodynamic and tissue models.

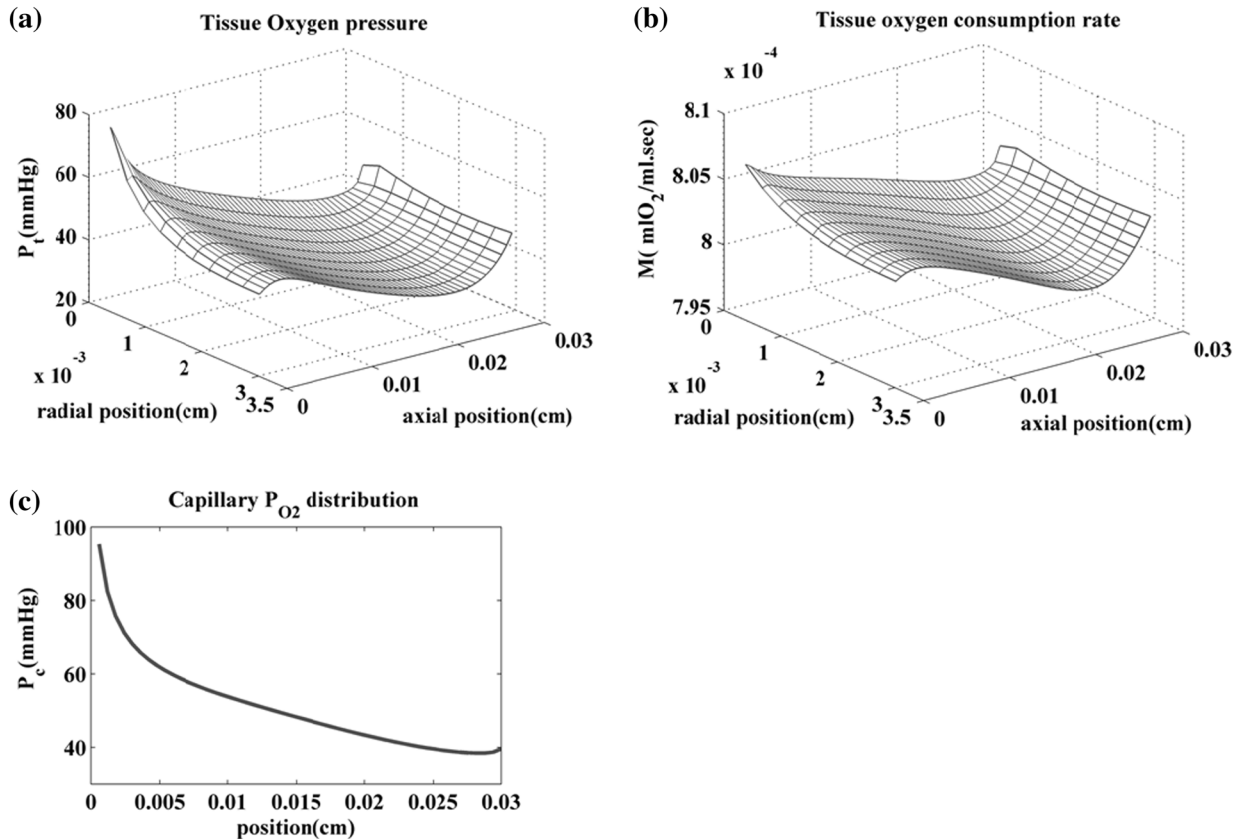


FIGURE 4. Steady state distribution in normal operation conditions of tissue oxygen partial pressure (a), Tissue oxygen consumption rate (b), and capillary oxygen distribution (c).

greater reduction in both average and minimum oxygen pressures.

Mean Tissue Oxygen Pressure Variation During Fluid Volume Replacement

To study the effect of the simultaneous changes of blood flow and hematocrit as it occurs during fluid resuscitation, a hemorrhagic trauma condition was simulated in the hemodynamic model.⁹ At steady state conditions, before bleeding, the total blood volume, hematocrit, and capillary blood flow were 5600 mL, 44%, and 7.7×10^{-9} mL/s, respectively. A class III bleeding condition was induced with a total blood loss of 33% followed by a short stabilization period. Both hematocrit and blood flow decreased during hemorrhage. During stabilization hematocrit continued to decrease but blood flow showed a small increase, Fig. 3a. After the stabilization period, fluid therapy was initiated using normal saline infusion at a rate of 80 mL/min. The simulated infusion continued until the normal capillary flow had been restored. During fluid

infusion the capillary flow increased while hematocrit decreased continuously. Contour plots in Figs. 7a and 7b show isobaric contours of mean and minimum oxygen partial pressure in the tissue as functions of blood flow and HCT. Pairs of values for capillary flow and HCT were taken from the hemodynamic response (Fig. 3a) and marked on the contour plots—triangles designate tissue average and minimum oxygen pressures during bleeding and circles designate these variables during fluid infusion. The temporal direction of the trajectories begins with the bleeding phase (triangles) on the higher right corner of the contours plot and progresses downward and to the left indicating reduction in blood flow and HCT as well as in oxygen partial pressure in the tissue. The infusion phase (circles) begins at the lower right side of the plot and progresses to the upper left corner, indicating increased blood flow with decreased HCT but also with continuing decrease of the oxygen partial pressure. Figure 7 indicates that increased blood flow may contribute to an increase in the tissues oxygen pressure but only if it is not accompanied by a significant decrease in HCT.

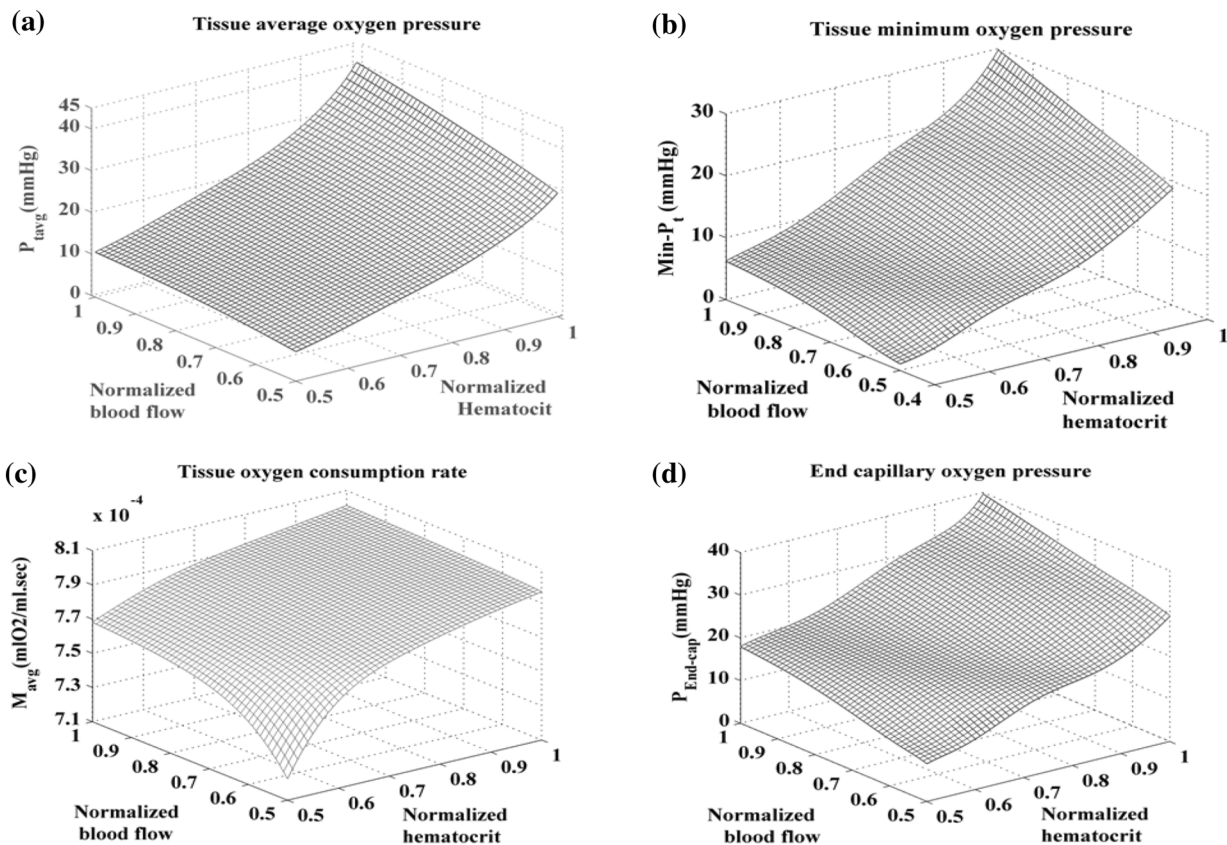


FIGURE 5. Tissue average oxygen pressure (a), tissue minimum oxygen pressure (b) tissue average oxygen consumption rate (c), and end-capillary oxygen pressure (d) with relative changes of hematocrit and blood flow. Results showed that tissue oxygenation is more sensitive to changes in hematocrit than blood flow for any combination of these variables.

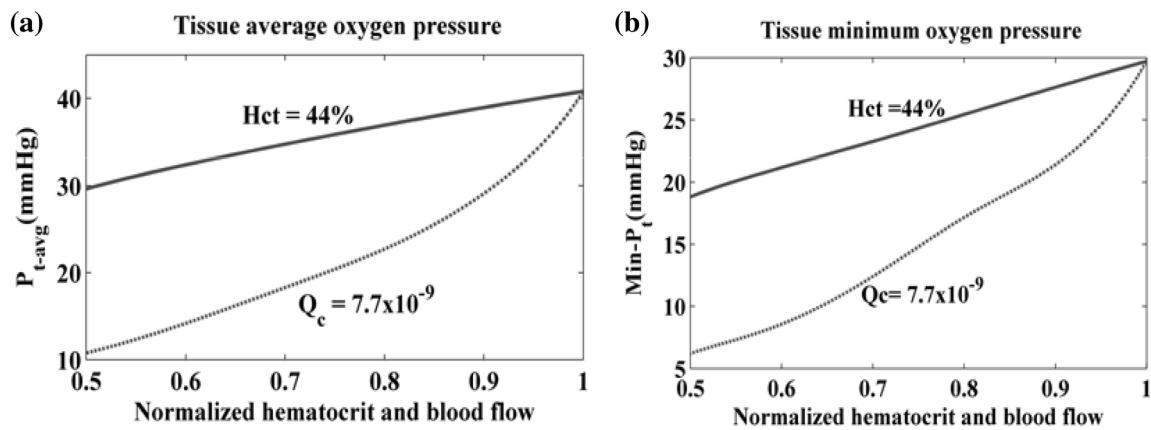


FIGURE 6. Tissue average (a) and minimum (b) oxygen pressures for normalized changes of capillary blood flow with hematocrit 44%, and normalized changes of hematocrit with blood flow 7.7×10^{-9} . Both Tissue average and minimum oxygen pressures were more sensitive to hematocrit than capillary blood flow.

DISCUSSION

The development of the capillary-tissue oxygen diffusion model was based on a modular design strategy. This allowed scalability and resolution variability in the simulation. Scalability refers to the ability to apply the same structure to various capillary and tissue dimensions without affecting the total number of sub-elements. Resolution variability refers to the ability to divide a capillary and tissue cylinder into a variable number of sub-elements. These two characteristics of the simulation allows to adapt the model to various tissues and supplying capillaries with the desired level of detail in the local oxygen content, consumption or inter-segment oxygen flow.

The number of underlying assumptions in the development of the oxygen flow model was reduced to allow more realistic values of oxygen diffusion to tissue. Also the cyclic boundary condition, where the venous end of a capillary group is in proximity to an arterial end of the next group allows interactions between capillaries. Several studies, such as those of Goldman and Bassingthwaite, presented models that were based on statistical distribution of capillaries while others presented an isolated capillary. This was an attempt to simplify the structure while maintaining the mutual effect of the capillaries.

Simulation runs of the hemodynamic model exhibited the hemodynamic response to hemorrhage and fluid therapy, Fig. 3. Results showed that the increase in capillary blood flow combined with decreased hematocrit resulted in an optimal point for oxygen delivery by blood independently of the infusion rate, as shown for the infusion rate of 40, 60, and 80 mL/min in Fig. 3. This raised the question: how is tissue oxygenation affected by the changes in capillary blood flow and hematocrit and whether the optimal point in oxygen delivery by blood corresponds to an optimal point in tissue oxygenation.

For normal conditions, the results showed higher oxygen pressure at the proximal regions in both axial and radial directions of the first third segment of the tissue cylinder (Fig. 4b). This was mainly due to the higher oxygen extraction at the initial segment of the capillary where the capillary oxygen concentration gradient was higher. Consequently, oxygen content of the capillary decreased rapidly in the axial direction due to the strong diffusion rate at the arterial side (Fig. 4c). The Michaelis–Menten consumption dynamics resulted in higher sustained consumption rate at this tissue region (Fig. 4b). Thus, a higher oxygen flux was necessary to cope with this need.

Moreover, results showed that the spatial distributions of oxygen partial pressure and consumption rate inside the tissue cylinder were not homogenous and have regions with maximum and minimum oxygen content in both axial and radial directions (Figs. 4a and 4b). This augments the importance of using 2D and 3D models in studying tissue oxygen deficiencies, such as tissue hypoxia and anoxia, in which oxygen content is not enough to cope with oxygen demand. Results (Figs. 4a and 4c) also showed that oxygen diffused from the arterial-end of a tissue cylinder to the venous-end of the preceding one and from the venous-end of the tissue cylinder into the venous-end of the capillary. This oxygen flux improved the oxygen content of the venous-end of both capillary and tissue cylinder. Therefore, it may be inexact to assume that the minimum tissue oxygen content occurs at the venous-end. We found, comparing our model to those of Li *et al.*,¹³ Dash *et al.*,⁴ and Sharan *et al.*²¹ that they showed that tissue oxygen pressure increases with increasing blood flow and hematocrit, as predicted by our model, but they did not determine the actual axial and radial distribution of oxygen pressure inside the tissue cylinder. Therefore, their conclusions regarding

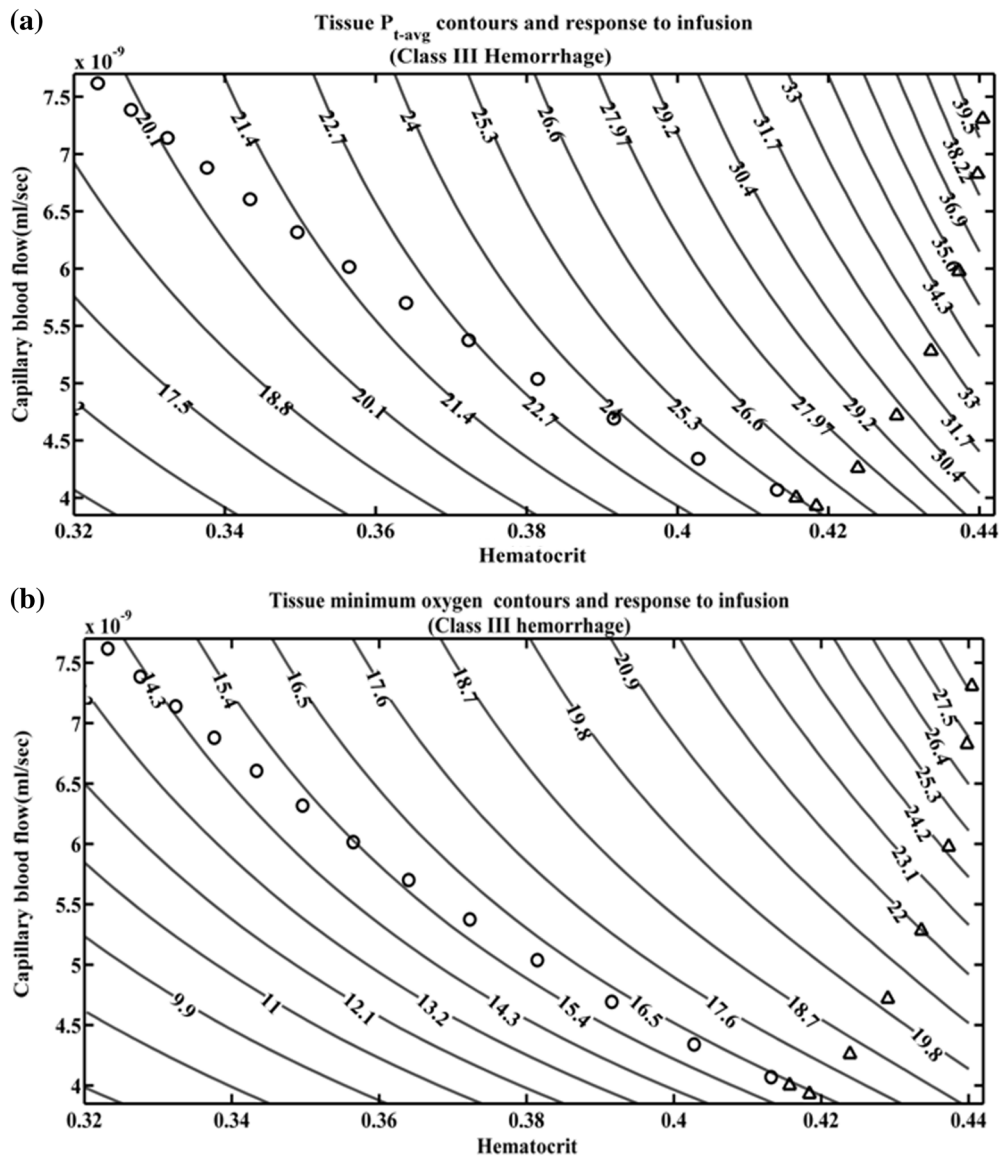


FIGURE 7. Hematocrit-capillary flow trajectories, during hemorrhage (triangles) and fluid therapy (circles), overlapped to tissue average (a) and minimum (b) oxygen pressure contours (mmHg). Results showed that both tissue average and minimum oxygen pressures deteriorated continuously during hemorrhage and fluid therapy.

the existence of hypoxic and anoxic regions may be inaccurate because they implicitly assumed a homogeneous radial oxygen distribution. Moreover, our model showed the importance of the oxygen flow among neighboring tissue cylinders on tissue oxygenation as observed by Dash and Bassingthwaite. In fact, this flow is an important oxygen source that improves the tissue venous-end oxygen pressure.

Simulation results showed that autoregulation is beneficial when raising the capillary blood flow with fixed oxygen concentration to improved tissue oxygenation (Figs. 5 and 6). The same figures show that infusion of blood oxygen carriers in certain pathological conditions, maintaining fixed blood flow, can improve tissue oxygenation. Both these results are in agreement

with the observations of Schumacher and Samsel.¹⁹ In fact, they found that lower oxygen concentration, produced by anemia or hypoxemia, without reduction of blood flow, and lower blood flow without anemia or hypoxemia can deteriorate tissue oxygenation. Moreover, Figs. 5 and 6 show that increasing the concentration of oxygen carriers is more effective in improving tissue oxygenation than increasing blood flow. Similar results were observed by Goldman *et al.*⁷ in their simulation for tissue oxygen pressure in sepsis. They found that hemoglobin oxygen saturation and consequently oxygen content is more important than red blood cells velocity in improving tissue oxygenation. The results are also in-line with the general belief that tissue oxygen uptake is a diffusion limited process and oxygen

extraction is determined by the metabolic activity rather than the oxygen delivery rate.

The worst oxygen consumption rate was obtained when blood flow and hematocrit changed simultaneously toward very small values, a condition that can occur in the case of unplanned fluid therapy of uncontrolled hemorrhage. Under this condition, tissue oxygen consumption rate deteriorated very quickly (Fig. 5c) due to the nature of Michaelis–Menten consumption dynamic.

Infusion of crystalloids and colloids fluids following hemorrhage increases blood flow. It is perceived as restoration of the circulation and improvement of oxygen delivery rate (D_{O_2}) to the tissue, Fig. 3. However, according to our previous study,²⁴ which was integrated with the tissue model in this study, this is true to a certain extent. In fact, continuing fluid infusion beyond the point of maximum oxygen delivery may be harmful due to the continuing drop in oxygen delivery by blood (D_{O_2}). Therefore, according to our model, restoring hemodynamic stability, in clinical settings, using crystalloids and colloids fluids should be limited to maintain the advantages of fluid therapy on oxygen transport. The integration of the hemodynamic and tissue models showed that, although fluid therapy seems to contribute to an increase in oxygen transport by blood up to a maximum point,²⁴ analysis of tissue oxygenation reveals that tissue oxygenation is improved only when blood oxygen concentration is preserved. Simulation results showed that, although the oxygen delivery rate improved at the initiation of fluid infusion, the trajectories of hematocrit and capillary flow generated by fluid therapy, Fig. 7, cause a continuous decrease of tissue average and minimum oxygen pressures. This is due to the high sensitivity of oxygen diffusion between capillary and tissue to oxygen concentration in blood. Therefore, based on model predictions, fluid therapy with solutions that do not include oxygen carriers will restore the circulation but will not maintain oxygen partial pressure in the tissue, Fig. 7.

In occlusion, results show that fluid resuscitation with crystalloids and colloids fluid can adversely affect tissue oxygenation. Our findings are in-line with the conclusions of several medical and biomedical engineering studies. For example, Knotzer *et al.*,¹⁰ showed that oxygen supply to the intestine was impaired in animals receiving lactated Ringer's solution after hemorrhagic shock. Funk and Baldinger⁵ showed that in a hamster model, capillary perfusion and tissue oxygenation were significantly depressed in lactated Ringer's hemodiluted animals. The same observations were shown in human studies by Lang *et al.*¹² Hußmann *et al.*,⁹ reviewed data from 35,664 patients recorded in the Trauma Registry of the German Society for Trauma Surgery (DGU). One remarkable finding of this study is that higher replacement volumes (crystalloids and colloids) in prehospital therapy were related to a significantly more frequent occurrence of organ failure and sepsis. Moreover, they found that the patient group receiving high volume replacement therapy required more extensive therapeutic care and more units of packed red blood cells.

CONCLUSIONS

A mathematical model was developed based on capillary proximity and fewer constraints. The model was used to compute the distribution of oxygen partial pressure in the supplying capillary and oxygen distribution and consumption rate in a tissue cylinder. It was also used to study the effect of blood flow and hematocrit on tissue oxygen content. Simulation results showed that oxygen content in the tissue was continuously compromised by blood dilution during fluid infusion and that the effect of hematocrit on tissue oxygenation is greater than the effect of blood flow.

APPENDIX

See Table 1.

TABLE 1. Parameters of capillary and tissue models.

Sym.	Meaning	Value	Refs.
R_c	Capillary radius	3.24×10^{-4} cm	22
L	Capillary, tissue cylinder length	0.03 cm	14
R_t	Tissue cylinder radius	3.25×10^{-3} cm	22
α_c	Blood oxygen solubility	3×10^{-5} mL O_2 /mL mmHg	20
α_t	Tissue oxygen solubility	3×10^{-5} mL O_2 /mL mmHg	20
D_t	Tissue oxygen diffusion	1.7×10^{-3} cm ² /s	20
k_t	Mass transfer coefficient	4.4×10^{-6} mL O_2 /(cm ² s mmHg)	21
Hb_{RBC}	Hemoglobin density	34 g/dl	8
$O_{2_{Hb}}$	Hemoglobin O_2 content	1.34 mL O_2 /g	8
N	Capillary and tissue axial divisions	50	
V	Tissue radial elements	10	

CONFLICT OF INTEREST

No benefits in any form have been or will be received from a commercial party related directly or indirectly to the subject of this manuscript.

STATEMENT OF HUMAN STUDIES

The work did not involve human subjects or human embryonic stem cells.

STATEMENT OF ANIMAL STUDIES

The work did not involve animal experiments or made use of tissues and cells.

REFERENCES

- ¹American College of Surgeons. Advanced Trauma Life Support for Doctors (8th ed.). Chicago: American College of Surgeons, 2008.
- ²Barnea, O., and N. Sheffer. A computer model for analysis of fluid resuscitation. *Comput. Biol. Med.* 23:443–454, 1993.
- ³Bickell, W., *et al.* Immediate versus delayed fluid resuscitation for hypotensive patients with penetrating torso injuries. *N. Engl. J. Med.* 331:1105–1109, 1994.
- ⁴Dash, R., and J. Bassingthwaite. Simultaneous blood-tissue exchange of oxygen, carbon dioxide, bicarbonate, and hydrogen ion. *Ann. Biomed. Eng.* 34(7):1129–1148, 2006.
- ⁵Funk, W., and V. Baldinger. Microcirculatory perfusion during volume therapy. A comparative study using crystalloid or colloid in awake animals. *Anesthesiology* 82:975–982, 1995.
- ⁶Goldman, D. Theoretical models of microvascular oxygen transport to tissue. *Microcirculation* 15(8):795–811, 2008.
- ⁷Goldman, D., *et al.* Effect of decreased O₂ supply on skeletal muscle oxygenation and O₂ consumption during sepsis: role of heterogeneous capillary spacing and blood flow. *Am. J. Physiol. Heart Circ. Physiol.* 290:2277–2285, 2006.
- ⁸Guyton, C., and J. Hall. Textbook of Medical Physiology (11th ed.). Philadelphia: Elsevier Saunders, 2006.
- ⁹Hußmann, B., *et al.* Influence of prehospital fluid resuscitation on patients with multiple injuries in hemorrhagic shock in patients from the DGU trauma registry. *J. Emerg. Trauma Shock* 4(4):465–471, 2011.
- ¹⁰Knotzer, H., *et al.* Comparison of lactated Ringer's, gelatine and blood resuscitation on intestinal oxygen supply and mucosal tissue oxygen tension in haemorrhagic shock. *Br. J. Anaesth.* 97(4):509–516, 2006.
- ¹¹Krogh, A. The number and distribution of capillaries in muscles with calculations of the oxygen pressure head necessary for supplying the tissue. *J. Physiol.* 52:409–415, 1919.
- ¹²Lang, K., *et al.* Colloids versus crystalloids, tissue oxygen tension in patients undergoing major abdominal surgery. *Anesth. Analg.* 93:405–409, 2001.
- ¹³Li, Z., *et al.* Nonlinear model for capillary-tissue oxygen transport and metabolism. *Ann. Biomed. Eng.* 25:604–619, 1997.
- ¹⁴Middleman, S. Transport Phenomena in the Cardiovascular System Wiley-Interscience Series on Biomedical Engineering, New York: Wiley, 1972.
- ¹⁵Morrison, C., *et al.* Hypotensive resuscitation strategy reduces transfusion requirements and severe postoperative coagulopathy in trauma patients with hemorrhagic shock: preliminary results of a randomized controlled trial. *J. Trauma* 70:652–663, 2011.
- ¹⁶National Institute for Clinical Excellence “NHS”, Prehospital Initiation of Fluid Replacement Therapy in Trauma, Issue 2004, National Institute for Clinical Excellence, 2007.
- ¹⁷Perel, P., *et al.*, Colloids versus crystalloids for fluid resuscitation in critically ill patients (Review). *Cochrane Database Syst. Rev.* 2, 2013.
- ¹⁸Popel, A. Theory of oxygen transport to tissue. *Crit. Rev. Biomed. Eng.* 17:257–321, 1989.
- ¹⁹Schumacker, P., and R. Samsel. Analysis of oxygen delivery and uptake relationships in the Krogh tissue model. *J. Appl. Physiol.* 67(3):1234–1244, 1989.
- ²⁰Sharan, M., *et al.* A compartmental model for oxygen transport in brain microcirculation. *Ann. Biomed. Eng.* 17(1):13–38, 1989.
- ²¹Sharan, M., *et al.* Parametric analysis of the relation between end-capillary and mean tissue PO₂ as predicted by a mathematical model. *J. Theor. Biol.* 195:439–449, 1998.
- ²²Sharan, M., *et al.* A two layer model for studying the effect of plasma on the delivery of oxygen to tissue using a finite element method. *Appl. Mater. Modelling* 21:419–426, 1997.
- ²³Shires, T., *et al.* Fluid therapy in haemorrhagic shock. *Arch. Surg.* 88:688–693, 1964.
- ²⁴Siam, J., *et al.* Optimization of oxygen delivery in fluid resuscitation for hemorrhagic shock: a computer simulation study. *Cardiovasc. Eng. Technol.* 5(1):82–95, 2014.
- ²⁵Wiggers, C. Experimental haemorrhage shock. In: Physiology of shock. New York: The Commonwealth Fund, 1950, pp. 121–143.
- ²⁶World Health Organization, Violence, Injuries, and Disabilities Biennial Report 2008–2009, WHO Library Cataloguing-in-Publication Data, 2010.